PRAMANA
— journal of
physics

Vol. 71, No. 1
July 2008
pp. 143–155

Effect of normal processes on thermal conductivity of germanium, silicon and diamond

BANASHREE SAIKIA[1,*] and ANIL KUMAR[2]
[1]Department of Physics, Icfai Tech., ICFAI University, P.O. Kamalghat, Agartala 799 210, India
[2]Department of Physics and Meteorology, Indian Institute of Technology, Kharagpur 721 302, India
[*]Corresponding author. E-mail: bulumoni_saikia@rediffmail.com

MS received 14 May 2007; revised 31 January 2008; accepted 4 March 2008

Abstract. The effect of normal scattering processes is considered to redistribute the phonon momentum in (a) the same phonon branch – KK-S model and (b) between different phonon branches – KK-H model. Simplified thermal conductivity relations are used to estimate the thermal conductivity of germanium, silicon and diamond with natural isotopes and highly enriched isotopes. It is observed that the consideration of the normal scattering processes involving different phonon branches gives better results for the temperature dependence of the thermal conductivity of germanium, silicon and diamond with natural and highly enriched isotopes. Also, the estimation of the lattice thermal conductivity of germanium and silicon for these models with the consideration of quadratic form of frequency dependences of phonon wave vector leads to the conclusion that the splitting of longitudinal and transverse phonon modes, as suggested by Holland, is not an essential requirement to explain the entire temperature dependence of lattice thermal conductivity whereas KK-H model gives a better estimation of the thermal conductivity without the splitting of the acoustic phonon modes due to the dispersive nature of the phonon dispersion curves.

Keywords. Phonon dispersion; phonon Boltzmann equation; lattice thermal conductivity; normal process; relaxation time; redistribution of phonon momentum.

PACS Nos 63.20.Kr; 63.20.Ry; 63.20.Dj

1. Introduction

Recent interest in semiconductor technologies and microelectronics [1] leads to the development of new materials possessing unusual physical properties. In modern microelectronics, the use of isotopically enriched crystals as substrates [2] for the integrated circuits can significantly increase the operational stability of the microprocessors by rapid removal of heat.

Callaway's [3] and Holland's model [4] have been used by Asen-Palmer *et al* [5] for the thermal conductivity analysis to estimate the effect of isotopes and normal

processes. Morelli *et al* [6] have later analysed the effect of isotopes on the thermal conductivity of group IV and III–V semiconductors by extending Callaway's model [3] to consider the contribution of transverse and longitudinal phonons separately. Recently, Kuleev and Kuleev [7] have considered the effects of normal phonon–phonon scattering processes on the thermal conductivity of Ge crystals with different isotopic compositions, by taking into account the redistribution of phonon momentum due to normal processes to each phonon oscillation branch [8] and between different phonon oscillation branches [9]. They observed that the redistribution between longitudinal and transverse phonons as described by Herring [9] leads to a significant suppression of drift motion and hence a drop in thermal conductivity.

It is therefore of our interest to appreciate different models of thermal conductivity analysis such as (i) Holland's model, which considers the dispersion effects of the transverse phonons, (ii) KK-S model, which does not consider the dispersion effect and (iii) KK-H model, which considers the redistribution of phonon momentum between different phonon oscillation branches due to normal processes. We compare the result of the temperature dependence of thermal conductivity values of Ge, Si and diamond, using these models. Experimental data used for comparison are (a) for natural and enriched Ge from Asen-Palmer *et al* [5], (b) for natural Si from Slack and Glassbrenner [10] and for enriched Si from Ruf *et al* [11] and (c) for natural and enriched diamond from Olson *et al* [12].

2. Lattice thermal conductivity

We use the method of Kuleev and Kuleev [7] to obtain different relations for the thermal conductivity from the solutions of phonon Boltzmann equation [3]. The phonon conductivity relation finally obtained is

$$K(T) = \sum_{\lambda} \frac{k_{\mathrm{B}}}{6\pi^2 C_\lambda} \left(\frac{k_{\mathrm{B}}T}{\hbar}\right)^3 \int_0^{\theta_{\mathrm{D}\lambda}/T} \tau_\alpha \frac{x^4 \mathrm{e}^x \mathrm{d}x}{(\mathrm{e}^x - 1)^2} \tag{1}$$

with

$$\tau_\alpha = \tau_{\mathrm{C}}^\lambda \left(1 + \frac{\beta_\alpha}{\tau_{\mathrm{N}}^\lambda}\right); \quad \beta_\alpha = \beta_{\mathrm{S}} = \frac{I_{\mathrm{N}}^\lambda}{I_{\mathrm{NR}}^\lambda};$$

$$\beta_\alpha = \beta_{\mathrm{H}} = \left(\frac{C_{\mathrm{L}}}{C_\lambda}\right)^2 \frac{I_{\mathrm{N}}^{\mathrm{L}} + 2C_*^3 I_{\mathrm{N}}^{\mathrm{T}}}{I_{\mathrm{NR}}^{\mathrm{L}} + 2C_*^5 I_{\mathrm{NR}}^{\mathrm{T}}} \quad \text{and} \quad x = \frac{\hbar\omega_{q\lambda}}{k_{\mathrm{B}}T}$$

and other expressions as given in table 1.

Here, the effective relaxation time τ_α has the second term taking care of the N-processes, which can result either from intra (Simon mechanism) or inter (Herring mechanism) branch redistribution of phonons. For Simon mechanism eq. (1) reduces to Callaway's thermal conductivity integral which involves β_{S} whereas, for Herring mechanism, the thermal conductivity integral involves β_{H}, the inter-branch phonon momentum redistribution mechanism, of N-processes.

Table 1. Summary of the models: for all the models $L_{\rm E} = \left[\frac{1}{L_{\rm C}}\frac{1-P}{1+P} + \frac{1}{l}\right]^{-1}$ is the effective phonon mean free path, $L_{\rm C} = 1.12\sqrt{ab}$ is the Casimir length, l is the length of the sample, a and b are the sample widths and ab is the cross-section. Also, $m = \frac{k_{\rm B}}{\hbar}$, $B^{\lambda}_{\rm N} = \frac{\hbar\gamma^2_{\lambda}}{Ma^2\theta^5_{\lambda}}$ and $B^{\lambda}_{\rm U} = \frac{\hbar\gamma^2_{\lambda}}{Ma\theta^2_{\lambda}}$ for all cases.

$\beta_\alpha = \beta_{\rm S} = 0$ Holland model $K(T) = K_{\rm L} + 2(K_{\rm TO} + K_{\rm TU})$	$\beta_\alpha = \beta_{\rm S} \neq 0$ KK-S model $K(T) = K_{\rm L} + 2K_{\rm T}$	$\beta_\alpha = \beta_{\rm H} \neq 0$ KK-H model $K(T) = K_{\rm L} + 2K_{\rm T}$
$K_{\rm L} = \frac{1}{3}S_{\rm L}T^3\int_0^{\theta_3/T}\tau^{\rm L}_{\rm C}(x)I(x){\rm d}x$	$K_{\rm L}(T) = \frac{1}{3}S_{\rm L}(I^{\rm L}_{\rm C} + \frac{(I^{\rm L}_{\rm N})^2}{I^{\rm L}_{\rm NR}})$	$K_{\rm L}(T) = \frac{1}{3}\frac{k_{\rm B}}{2\pi^2 C_{\rm L}}(\frac{k_{\rm B}T}{\hbar})^3\ (I^{\rm L}_{\rm C} + \frac{(I^{\rm L}_{\rm N})^2 + 2C^3_* I^{\rm L}_{\rm N} I^{\rm T}_{\rm N}}{I^{\rm L}_{\rm NR} + 2C^5_* I^{\rm T}_{\rm NR}})$
$K_{\rm TO} = \frac{1}{3}S_{\rm TO}T^3\int_0^{\theta_1/T}\tau^{\rm TO}_{\rm C}(x)I(x){\rm d}x$	$K_{\rm T}(T) = \frac{1}{3}S_{\rm T}(I^{\rm T}_{\rm C} + \frac{(I^{\rm T}_{\rm N})^2}{I^{\rm T}_{\rm NR}})$	$K_{\rm T}(T) = \frac{1}{3}\frac{k_{\rm B}}{2\pi^2 C_{\rm T}}(\frac{k_{\rm B}T}{\hbar})^3\ (I^{\rm T}_{\rm C} + \frac{I^{\rm L}_{\rm N} I^{\rm T}_{\rm N} + 2C^3_*(I^{\rm T}_{\rm N})^2}{I^{\rm L}_{\rm NR} + 2C^5_* I^{\rm T}_{\rm NR}}(\frac{C_{\rm L}}{C_{\rm T}})^2)$
$K_{\rm TU} = \frac{1}{3}S_{\rm TU}T^3\int_{\theta_1/T}^{\theta_2/T}\tau^{\rm TU}_{\rm C}(x)I(x){\rm d}x$	–	–
$S_\lambda = \frac{k_{\rm B}}{2\pi^2 C_\lambda}(\frac{k_{\rm B}}{\hbar})^3$	$I^{\lambda}_{\rm C} = \int_0^{\theta_\lambda/T}\tau^{\lambda}_{\rm C}\frac{x^4{\rm e}^x{\rm d}x}{({\rm e}^x-1)^2}$	$I^{\lambda}_{\rm C} = \int_0^{\theta_\lambda/T}\tau^{\lambda}_{\rm C}\frac{x^4{\rm e}^x{\rm d}x}{({\rm e}^x-1)^2}$
$I(x) = \frac{x^4{\rm e}^x{\rm d}x}{({\rm e}^x-1)^2}$	$I^{\lambda}_{\rm N} = \int_0^{\theta_\lambda/T}\frac{\tau^{\lambda}_{\rm C}}{\tau^{\lambda}_{\rm N}}\frac{x^4{\rm e}^x{\rm d}x}{({\rm e}^x-1)^2}$	$I^{\lambda}_{\rm N} = \int_0^{\theta_\lambda/T}\frac{\tau^{\lambda}_{\rm C}}{\tau^{\lambda}_{\rm N}}\frac{x^4{\rm e}^x{\rm d}x}{({\rm e}^x-1)^2}$
$\tau^{\rm L}_{\rm C} = [\frac{C_{\rm L}}{L_{\rm E}} + A^{\rm L}_{\rm I}m^4x^4T^4 + B^{\rm L}_{\rm N}m^2x^2T^5]^{-1}$	$I^{\lambda}_{\rm NR} = \int_0^{\theta_\lambda/T}\frac{\tau^{\lambda}_{\rm C}}{\tau^{\lambda}_{\rm N}\tau^{\lambda}_{\rm R}}\frac{x^4{\rm e}^x{\rm d}x}{({\rm e}^x-1)^2}$	$I^{\lambda}_{\rm NR} = \int_0^{\theta_\lambda/T}\frac{\tau^{\lambda}_{\rm C}}{\tau^{\lambda}_{\rm N}\tau^{\lambda}_{\rm R}}\frac{x^4{\rm e}^x{\rm d}x}{({\rm e}^x-1)^2}$
$\tau^{\rm TO}_{\rm C} = [\frac{C_{\rm TO}}{L_{\rm E}} + A^{\rm T}_{\rm I}m^4x^4T^4 + B^{\rm T}_{\rm N}mxT^5]^{-1}$	$\tau^{\lambda}_{\rm C} = [(\tau^{\lambda}_{\rm N})^{-1} + (\tau^{\lambda}_{\rm R})^{-1}]^{-1}$	$\tau^{\lambda}_{\rm C} = [(\tau^{\lambda}_{\rm N})^{-1} + (\tau^{\lambda}_{\rm R})^{-1}]^{-1}$
$\tau^{\rm TU}_{\rm C} = [\frac{C_{\rm TU}}{L_{\rm E}} + A^{\rm T}_{\rm I}m^4x^4T^4 + \frac{B^{\rm T}_{\rm U}m^2x^2T^2}{\sinh x}]^{-1}$	$(\tau^{\lambda}_{\rm R})^{-1} = C_\lambda/L_{\rm E} + A^{\lambda}_{\rm I}m^2x^4T^4 + B^{\lambda}_{\rm U}m^2x^2T^3{\rm e}^{-\theta_\lambda/3T}$	$(\tau^{\lambda}_{\rm R})^{-1} = C_\lambda/L_{\rm E} + A^{\lambda}_{\rm I}m^4x^4T^4 + B^{\lambda}_{\rm U}m^2x^2T^3{\rm e}^{-\theta'_{\rm D}/3T}$
	$(\tau^{\rm L}_{\rm N})^{-1} = B^{\rm L}_{\rm N}m^2x^2T^5$	$(\tau^{\rm L}_{\rm N})^{-1} = B^{\rm L}_{\rm N}m^2x^2T^5$
	$(\tau^{\rm T}_{\rm N})^{-1} = B^{\rm T}_{\rm N}mxT^5$	$(\tau^{\rm T}_{\rm N})^{-1} = B^{\rm T}_{\rm N}mxT^5$
		$C_* = \frac{C_{\rm L}}{C_{\rm T}}$

3. Thermal conductivity relations

We now analyse the effect of isotopes on three different materials, viz., Ge, Si and diamond using eq. (1) for different models which can be derived by substituting the terms β_S and β_H.

3.1 *Holland model* ($\beta_\alpha = \beta_S = 0$) (*with splitting of transverse mode*)

In eq. (1), if we consider $\beta_\alpha = \beta_S = 0$, i.e., if we neglect the effects of normal processes, the thermal conductivity integral reduces to an expression similar to Holland's model. Various parameters used for calculation are listed in table 2. From the calculations, shown in figures 1a, 2a and 3a, we observe that the temperature dependences of the thermal conductivity of Ge, Si and diamond (for natural isotopes and enriched isotopes) are estimated in a better way at low temperatures as compared to high temperatures. The transverse phonons responsible for umklapp processes are observed to carry thermal energy at high temperatures assisted by longitudinal phonons.

3.2 *KK-S model* (*Simon mechanism* $\beta_\alpha = \beta_S \neq 0$)

In eq. (1) if we consider $\beta_\alpha = \beta_S$, it gives Morelli *et al*'s model [8] which is the modification to Callaway's model by considering the frequency and temperature dependencies for the umklapp and normal phonon scattering processes in terms of Grüneisen parameters and Debye temperatures. The thermal conductivity relations are summarized in table 1. We consider the longitudinal and transverse Grüneisen parameters to be adjustable parameters to get a best fit between theory and experiment. We use the model to estimate the temperature dependencies of thermal conductivities of Ge, Si and diamond as plotted in figures 1b, 2b and 3b with parameters given in table 2.

3.3 *KK-H model* (*Herring mechanism* $\beta_\alpha = \beta_H \neq 0$)

We analyse the effect of normal phonon processes on natural isotopes and isotopically enriched Ge, Si and diamond, substituting β_H in eq. (1). The modified thermal conductivity integrals are given in table 1. These relations clearly show that the thermal conductivity for either longitudinal phonons or transverse phonons depends on the conductivity integral of the same polarization along with the contribution from other polarization branches due to the effects of normal processes because of the cross polarization effect as suggested by Herring. We calculate and plot the thermal conductivity of Ge, Si and diamond, using the model along with the relaxation times for different phonon scattering processes, as shown in figures 1c, 2c and 3c.

4. Thermal conductivity estimation with splitting of acoustic phonon modes

We estimate the thermal conductivity of Ge and Si for three distinct cases:

1. Splitting of only transverse modes with KK-S model without distinction of phase and group velocities where longitudinal phonon mode is not dispersive.
2. Splitting of both longitudinal and transverse modes with KK-S model without distinction of phase and group velocities.
3. No splitting of the phonon modes with KK-S and KK-H models. Distinction of phase and group velocities is also considered with these approaches.

The splitting of the conductivity integrals can be done to the critical frequencies obtained from the phonon dispersion curves by assuming as the points of intersection of the two slopes on the dispersion curves at the low and high phonon frequency regions, i.e., ω_1 for the transverse phonons and ω_3 for the longitudinal phonons.

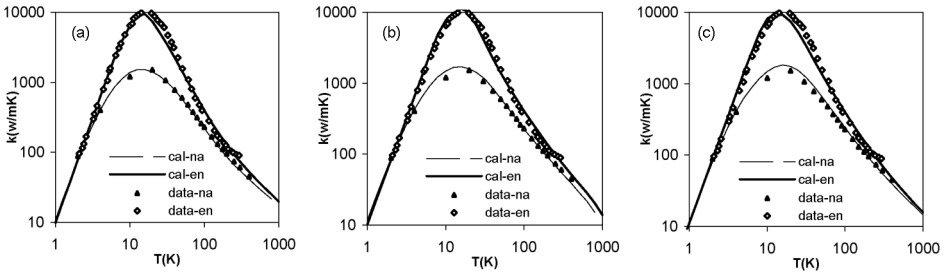

Figure 1. Thermal conductivity curves, calculated for (**a**) Holland model, (**b**) KK-S model and (**c**) KK-H model with the parameters given in tables 2a, 2b and 2c for Ge sample with natural and enriched isotopic composition. Experimental data are taken from ref. [3].

Table 2a. Transverse and longitudinal velocities, crystal volume and Debye temperatures.

Material	C_{TO} (m/s)	C_{TU} (m/s)	C_{L} (m/s)	V (m^3)	θ_{TO} (K)	θ_{TU} (K)	θ_{L} (K)
Ge (na)	3540	1300	4920	22.6×10^{-30}	101	118	333
Ge (en)	3540	1300	4920	22.6×10^{-30}	101	118	333
Si (na)	5850	2000	8430	19.9×10^{-30}	180	240	586
Si (en)	5850	2000	8430	19.9×10^{-30}	180	240	586
C (na)	12800	4200	17500	5.68×10^{-30}	1160	1233	1820
C (en)	12800	4200	17500	5.68×10^{-30}	1160	1233	1820

For $\beta = \beta_{\mathrm{S,H}}$ model $C_{\mathrm{TO}} = C_{\mathrm{T}}$ and $\theta_{\mathrm{TU}} = \theta_{\mathrm{T}}$.

Table 2b. Details of samples.

Material	Isotope composition	Γ	a (m)	b (m)	l (m)	L_{C} (m)	P	L_{E} (m)
Ge (na)	20.5% ^{70}Ge 27.4% ^{72}Ge 7.8% ^{73}Ge 36.5% ^{74}Ge 7.8% ^{76}Ge	6.08×10^{-4}	1.30×10^{-3}	1.30×10^{-3}	15.0×10^{-3}	1.66×10^{-3}	0.38	3.0×10^{-3}
Ge (en)	99.99% ^{70}Ge 0.01% ^{72}Ge	0.816×10^{-7}	2.20×10^{-3}	2.50×10^{-3}	44.5×10^{-3}	2.63×10^{-3}	0.19	3.6×10^{-3}
Si (na)	92.23% ^{28}Si 4.67% ^{29}Si 3.1% ^{30}Si	2.00×10^{-4}	1.30×10^{-3}	1.30×10^{-3}	0.2×10^{-3}	4.4×10^{-3}	0.06	4.0×10^{-3}
Si (en)	99.859% ^{28}Si 0.1272% ^{29}Si 0.014% ^{30}Si	2.33×10^{-6}	1.30×10^{-3}	1.30×10^{-3}	30.0×10^{-3}	2.37×10^{-3}	0.83	14.0×10^{-3}
C (na)	98.9% ^{12}C 1.1% ^{13}C	0.75×10^{-4}	–	–	–	–	–	$0.55\times10^{-3*}$
C (en)	99.93% ^{12}C 0.07% ^{13}C	4.86×10^{-6}	4.00×10^{-3}	3.00×10^{-3}	4.0×10^{-3}	3.87×10^{-3}	0.65	3.3×10^{-3}

*This parameter is taken from ref. [8]. Sample's dimension for Ge is taken from ref. [3], C-enriched sample is taken from ref. [5] and Si sample is taken from ref. [12].

Table 2c.

Model	Material	A_I^L (s^3)	A_I^T (s^3)	B_U^L (s/K)	B_U^T *(s) (s/K)	B_N^L (s/K^3)	B_N^T (K^{-4})
$\beta = 0$	Ge (na)	9.20×10^{-45}	2.40×10^{-44}	–	4.50×10^{-18}	9.00×10^{-24}	1.50×10^{-11}
	Ge (en)	1.23×10^{-48}	3.28×10^{-48}	–	4.50×10^{-18}	9.00×10^{-24}	1.50×10^{-11}
$\beta = \beta_S$	Ge (na)	9.20×10^{-45}	2.40×10^{-44}	1.4×10^{-19}	1.60×10^{-19}	4.70×10^{-24}	1.37×10^{-12}
	Ge (en)	1.23×10^{-48}	3.28×10^{-48}	1.4×10^{-19}	1.60×10^{-19}	4.70×10^{-24}	1.37×10^{-12}
$\beta = \beta_H$	Ge (na)	9.20×10^{-45}	2.40×10^{-44}	1.5×10^{-19}	1.65×10^{-19}	4.50×10^{-24}	1.22×10^{-12}
	Ge (en)	1.23×10^{-48}	3.28×10^{-48}	1.5×10^{-19}	1.65×10^{-19}	4.50×10^{-24}	1.22×10^{-12}
$\beta = 0$	Si (na)	5.29×10^{-46}	1.59×10^{-45}	–	9.95×10^{-18}	1.20×10^{-24}	9.60×10^{-13}
	Si (en)	6.16×10^{-48}	1.85×10^{-47}	–	9.95×10^{-18}	1.20×10^{-24}	9.60×10^{-13}
$\beta = \beta_S$	Si (na)	5.29×10^{-46}	1.59×10^{-45}	5.98×10^{-20}	1.00×10^{-19}	0.91×10^{-23}	1.40×10^{-12}
	Si (en)	6.16×10^{-48}	1.85×10^{-47}	5.98×10^{-20}	1.00×10^{-19}	0.91×10^{-23}	1.40×10^{-12}
$\beta = \beta_H$	Si (na)	5.29×10^{-46}	1.59×10^{-45}	6.80×10^{-20}	1.50×10^{-19}	2.00×10^{-23}	2.80×10^{-13}
	Si (en)	6.16×10^{-48}	1.85×10^{-47}	6.80×10^{-20}	1.50×10^{-19}	2.00×10^{-23}	2.80×10^{-13}
$\beta = 0$	C (na)	6.33×10^{-48}	1.62×10^{-47}	–	4.50×10^{-18}	2.10×10^{-25}	1.60×10^{-14}
	C (en)	4.10×10^{-49}	1.05×10^{-48}	–	4.50×10^{-18}	2.10×10^{-25}	1.60×10^{-14}
$\beta = \beta_S$	C (na)	6.33×10^{-48}	1.62×10^{-47}	11.6×10^{-21}	2.20×10^{-20}	4.80×10^{-26}	2.20×10^{-14}
	C (en)	4.10×10^{-49}	1.05×10^{-48}	11.6×10^{-21}	2.20×10^{-20}	4.80×10^{-26}	2.20×10^{-14}
$\beta = \beta_H$	C (na)	6.33×10^{-48}	1.62×10^{-47}	9.6×10^{-21}	1.90×10^{-20}	4.50×10^{-26}	2.00×10^{-14}
	C (en)	4.10×10^{-49}	1.05×10^{-48}	9.6×10^{-21}	1.90×10^{-20}	4.50×10^{-26}	2.00×10^{-14}

*For model $\beta = 0$, unit for B_U^T is s, otherwise s/K.

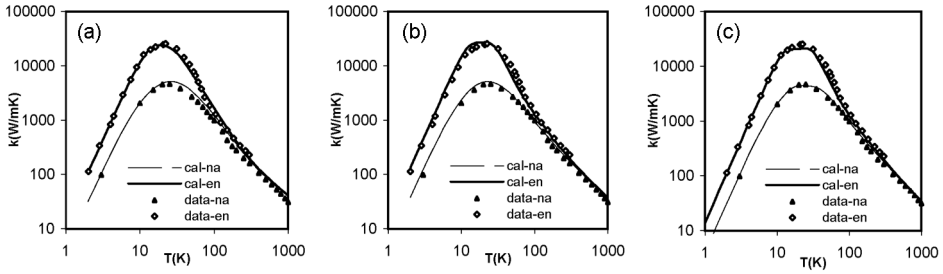

Figure 2. Thermal conductivity curves, calculated for (**a**) Holland model, (**b**) KK-S model and (**c**) KK-H model with the parameters given in tables 2a, 2b and 2c for Si sample with natural and enriched isotopic composition. Experimental data are taken from ref. [12].

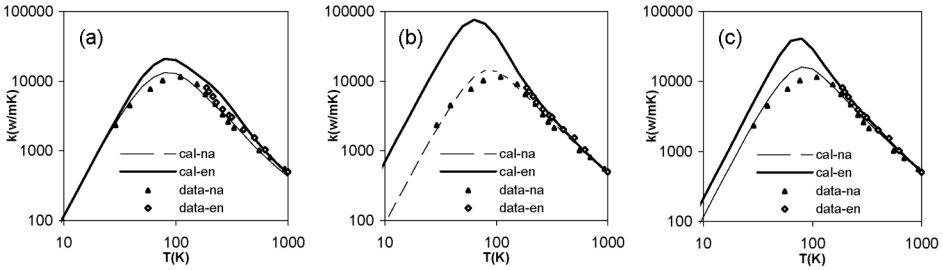

Figure 3. Thermal conductivity curves, calculated for (**a**) Holland model, (**b**) KK-S model and (**c**) KK-H model with the parameters given in tables 2a, 2b and 2c for diamond sample with natural and enriched isotopic composition. Experimental data are taken from ref. [5].

The conductivity integrals with splitting are given in eqs (2)–(4).

$$I_{\mathrm{C}}^{\mathrm{L}} = \int_0^{\theta_3/T} \tau_{\mathrm{C}}^{\mathrm{L}} I(x)\mathrm{d}x + \int_{\theta_3/T}^{\theta_4/T} \tau_{\mathrm{C}}^{\mathrm{L}} I(x)\mathrm{d}x,$$
$$I_{\mathrm{C}}^{\mathrm{T}} = \int_0^{\theta_1/T} \tau_{\mathrm{C}}^{\mathrm{T}} I(x)\mathrm{d}x + \int_{\theta_1/T}^{\theta_2/T} \tau_{\mathrm{C}}^{\mathrm{T}} I(x)\mathrm{d}x, \tag{2}$$

$$I_{\mathrm{N}}^{\mathrm{L}} = \int_0^{\theta_3/T} \frac{\tau_{\mathrm{C}}^{\mathrm{L}}}{\tau_{\mathrm{N}}^{\mathrm{L}}} I(x)\mathrm{d}x + \int_{\theta_3/T}^{\theta_4/T} \frac{\tau_{\mathrm{C}}^{\mathrm{L}}}{\tau_{\mathrm{N}}^{\mathrm{L}}} I(x)\mathrm{d}x,$$
$$I_{\mathrm{N}}^{\mathrm{T}} = \int_0^{\theta_1/T} \frac{\tau_{\mathrm{C}}^{\mathrm{T}}}{\tau_{\mathrm{N}}^{\mathrm{T}}} I(x)\mathrm{d}x + \int_{\theta_1/T}^{\theta_2/T} \frac{\tau_{\mathrm{C}}^{\mathrm{T}}}{\tau_{\mathrm{N}}^{\mathrm{T}}} I(x)\mathrm{d}x, \tag{3}$$

$$I_{\mathrm{NR}}^{\mathrm{L}} = \int_0^{\theta_3/T} \frac{\tau_{\mathrm{C}}^{\mathrm{L}}}{\tau_{\mathrm{N}}^{\mathrm{L}}\tau_{\mathrm{R}}^{\mathrm{L}}} I(x)\mathrm{d}x + \int_{\theta_3/T}^{\theta_4/T} \frac{\tau_{\mathrm{C}}^{\mathrm{L}}}{\tau_{\mathrm{N}}^{\mathrm{L}}\tau_{\mathrm{R}}^{\mathrm{L}}} I(x)\mathrm{d}x,$$
$$I_{\mathrm{NR}}^{\mathrm{T}} = \int_0^{\theta_1/T} \frac{\tau_{\mathrm{C}}^{\mathrm{T}}}{\tau_{\mathrm{N}}^{\mathrm{T}}\tau_{\mathrm{R}}^{\mathrm{T}}} I(x)\mathrm{d}x + \int_{\theta_1/T}^{\theta_2/T} \frac{\tau_{\mathrm{C}}^{\mathrm{T}}}{\tau_{\mathrm{N}}^{\mathrm{T}}\tau_{\mathrm{R}}^{\mathrm{T}}} I(x)\mathrm{d}x. \tag{4}$$

The effect of curvature of phonon dispersion can be further extended by describing the longitudinal and transverse velocities as [13]

$$q_{\mathrm{L}} = C_{\mathrm{L}}^{-1}\omega_{\mathrm{L}}(1 + \alpha\omega_{\mathrm{L}}) \tag{5}$$

$$q_{\mathrm{T}} = C_{\mathrm{T}}^{-1}\omega_{\mathrm{T}}(1 + \beta\omega_{\mathrm{T}}^2), \tag{6}$$

where

$$\alpha = \left(\frac{1}{\omega_{\mathrm{mL}}}\right)\left[\frac{C_{\mathrm{L}}}{\omega_{\mathrm{mL}}}(6n\pi^2)^{1/3} - 1\right]$$

and

$$\beta = \left(\frac{1}{\omega_{\mathrm{mT}}^2}\right)\left[\frac{C_{\mathrm{T}}}{\omega_{\mathrm{mT}}}(6n\pi^2)^{1/3} - 1\right],$$

where n is the number of lattice points per unit volume of the solids, ω_{mL} and ω_{mT} are the maximum values of the frequency of the phonon branches.

5. Results and discussion

The solutions of the phonon BTE require the detailed calculations of the phonon scattering cross-section which are carried out by the perturbation techniques. The frequency and temperature dependences of three-phonon processes are strongly influenced by the phonon branches and anharmonicity constants. In the analysis of Asen-Palmer *et al* [5] of the measured thermal conductivity of Ge crystals, they observed that in Holland model the splitting of the transverse branch at ω_1 (the frequency at which U-process starts) is not very essential as the inclusion of the correction term, K_2, with splitting not giving an improved agreement with the experimental results. We, therefore, calculate the thermal conductivity of Ge with natural and enriched isotopes at different temperatures using (a) Holland model without the correction term, but with the splitting of transverse acoustic branch, (b) KK-S model, which includes the correction term, considering the normal scattering on the same branch but without the splitting of the transverse acoustic branch, and (c) KK-H model, which includes the correction term without the splitting of the transverse acoustic branch.

We assume that the coupling parameters for the longitudinal and the transverse three-phonon scattering processes for N- and U-processes depend on the Grüneisen parameter and the Debye characteristic temperature which are derived from the anharmonicity of the crystal. These parameters, viz., B_{N}^{λ} and B_{U}^{λ} depend on the mass of the crystal; not on the mass fluctuations due to isotopes. Thus we consider the same values of these parameters to estimate the temperature dependence of thermal conductivity and compare the theoretical results with the experimental results as listed in table 2. We observe that with Holland model the values of the parameters B_{N}^{λ} and B_{U}^{λ} are different as compared to those with the other two approaches. The contribution of the U-processes in the Holland model gives a better agreement at higher temperatures as compared to that at temperatures above the

thermal conductivity maximum, where N-processes contribute strongly along with the isotope scattering. Figures 1a, 2a and 3a also show that the agreement is reasonably good for diamond and Ge as compared to Si. Secondly, the analysis also leads to the fact that the isotopic scattering parameter A is different for highly enriched isotopes as compared to the natural isotopes which is obvious from the observations as the thermal conductivity maximum gives a large magnitude of $K(T)$ for highly enriched isotopes. The magnitude of the ratio $(A_{\rm na}/A_{\rm en})$ is almost equal to the mass fluctuation factor Γ.

The analysis of the thermal conductivity of Ge with natural and enriched isotopes shows that the Holland model gives reasonably good agreement between theory and experiment for the temperature dependence of the thermal conductivity in the entire temperature range of 1–1000 K. However, the normal scattering processes underestimate the thermal conductivity above the thermal conductivity maximum as shown in figure 1a. In figure 1b the temperature dependence of thermal conductivity, calculated using KK-S model shows that the N-processes contribute more as compared to the U-processes as the thermal conductivity curve goes down the experimental curve in the temperature region where U-processes mainly contribute the thermal conductivity. With KK-H model, figure 1c shows that the agreement between theory and experiment is better for Ge with natural isotopes as compared to highly enriched isotopes. This may be due to the fact that the isotope scattering and normal scattering processes contribute simultaneously at temperatures above maximum thermal conductivity which may lead to enhancement of the N-processes.

For Si, figures 2a, 2b and 2c clearly show that the thermal conductivity of Si gets enhanced when enriched isotopically. It can be explained by the change $A_{\rm en}$ from $A_{\rm na}$ by the order of 1.1×10^{-2} which is the same as the change in Γ as observed for Ge. The agreement is better for natural Si as compared to highly enriched isotopes. This is due to the enhancement of the N-processes due to isotopes which yield lower theoretical values above the thermal conductivity maximum. The contribution of U-processes to the thermal conductivity in Holland model and KK-S model is high as compared to KK-H model because in KK-H model U-processes weaken and the agreement between theoretical results and experimental measurements is reasonably good. Values of different parameters listed in table 2 clearly show that combination of N- and U-processes explain the temperature dependence of the thermal conductivity of different crystals with isotope compositions.

Figure 3a represents the analysis with Holland model for diamond with natural and highly enriched isotopes. The agreements are good at room temperature for highly enriched isotopes. However, for diamond with natural isotopes, there occurs a deviation below the maximum thermal conductivity. It may be due to the strong contribution of N-processes in the presence of isotopes. The agreement at higher temperatures above the maximum thermal conductivity is reasonably good. The calculations with the KK-S model gives comparatively good agreement at higher temperatures but deviations around the maximum thermal conductivity suggest that both Holland and KK-S models consider the contribution of the transverse phonon as shown in figures 3a and 3b. Finally, in figure 3c the agreement between theory and experiment for natural and highly enriched isotopes is qualitatively better with KK-H model as compared to other two models, i.e. Holland and KK-S models. It may be due to the fact that the redistribution of phonon momentum

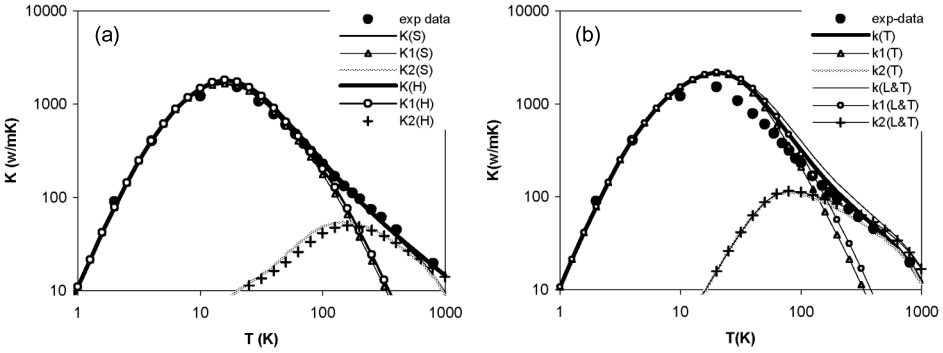

Figure 4. (**a**) Temperature dependence of lattice thermal conductivity for natural Ge with KK-S model. Longitudinal and transverse modes are considered separately with the splitting of frequency in both transverse and longitudinal modes. T denotes the splitting of transverse only and L&T denotes the splitting of both transverse and longitudinal. (**b**) Comparison of lattice thermal conductivity for natural Ge with KK-S model (S) and KK-H model (H). The contributions of K_1 and K_2 are shown separately.

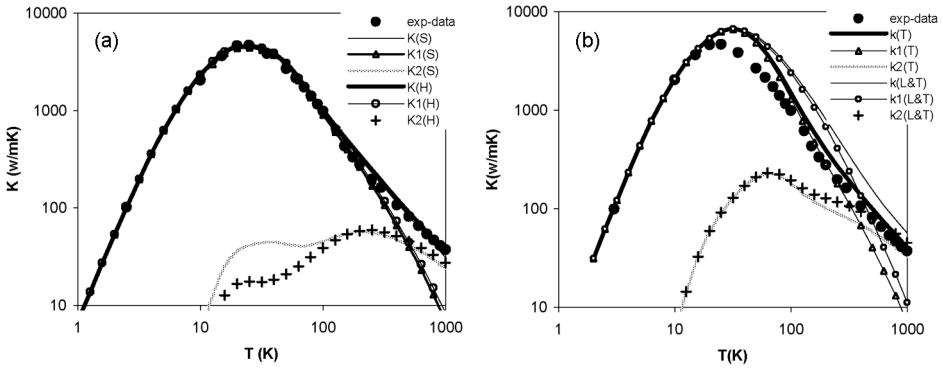

Figure 5. (**a**) Temperature dependence of lattice thermal conductivity for natural Si with KK-S model. Longitudinal and transverse modes are considered separately with the splitting of frequency in both transverse and longitudinal modes. T denotes the splitting of transverse only and L&T denotes the splitting of both transverse and longitudinal. (**b**) Comparison of lattice thermal conductivity for natural Si with KK-S model (S) and KK-H model (H). The contributions of K_1 and K_2 are shown separately.

across the phonon branches for N-processes weakens the U-processes. The curve fitting procedure gives additional information that the presence of higher concentration of isotopes enhances the normal three-phonon scattering processes.

The thermal conductivity for (i) the splitting of only transverse mode and (ii) the splitting of both transverse and longitudinal modes with KK-S model is shown in figure 4a. The calculations show that the splitting of only transverse mode gives better fit as compared to the splitting of both the longitudinal and transverse

Table 3a. Values of parameters for natural Ge and Si used in calculation includes transverse and longitudinal Debye temperatures and transverse and longitudinal velocities.

Material	θ_{LO} (K)	θ_{LU} (K)	θ_{TO} (K)	θ_{TU} (K)	C_{LO} (m/s)	C_{LU} (m/s)	C_{TO} (m/s)	C_{TU} (m/s)	α	β
Ge (na)	192	333	101	118	4920	2460	3540	1300	5.62×10^{-15}	6.43×10^{-27}
Si (na)	350	586	180	240	8430	4240	3850	2000	1.56×10^{-15}	1.24×10^{-27}

Table 3b. Values of parameters for natural Ge and Si used in calculation includes phonon–isotope, phonon–phonon umklapp and phonon–phonon normal scattering rate coefficients for transverse and longitudinal phonons.

Material	A_I^L (s^3)	A_I^T (s^3)	B_U^L (s/K)	B_U^T (s/K)	B_N^L (s/K^3)	B_N^T (K^{-4})
Ge (na)	9.20×10^{-45}	2.40×10^{-44}	1.5×10^{-19}	1.65×10^{-19}	4.5×10^{-24}	1.22×10^{-12}
Si (na)	5.29×10^{-46}	1.59×10^{-45}	6.8×10^{-20}	1.50×10^{-19}	0.2×10^{-24}	2.80×10^{-13}

phonon modes. This can be due to the enhancement of thermal conductivity by the additional splitting of the longitudinal phonon mode. The parameters listed in table 3 are adjusted to fit the thermal conductivity results. In figure 4b, we compare the thermal conductivity results for the KK-S and KK-H models without splitting the phonon modes and observe that the KK-H model gives reasonably good agreement between theory and experiment. The thermal conductivity curves for the correction term K_2 along with the conductivity curves K_1 are also shown in figure 4b. We also analyse the thermal conductivity of Si with isotopes and plot the curves in figures 5a and 5b. We observe that the results are similar to what we observe for the thermal conductivity of Ge with isotopes. The parameters used in the calculations are listed in table 3. The agreement between theory and experiment is again reasonably good for KK-H model. This can be due to the fact that KK-H model combines most of the merits of the other models, i.e., it contains (a) the effect of the dispersive nature of the transverse mode due to the phonon momentum transfer across the polarization, (b) the effect of the normal processes which are also enhanced due to the presence of the isotopes, (c) the contribution of the longitudinal and transverse phonons separately and (d) incorporation of phonon velocities as a function of frequency. From these calculations, it is observed that KK-H model can be used for the thermal conductivity analysis which combines the effects of normal processes and the dispersive phonon modes without considering the splitting of phonon modes.

References

[1] K Schwab, E A Henriksen, J M Worlock and M L Roukes, *Nature (London)* **404**, 974 (2000)

[2] M S Dresselhaus, Y M Lin, S B Cronin, O Rabin, G Dreuelhaus and T Koga, *Semicond. Semimetals* **71**, 1 (2001)

[3] J Callaway, *Phys. Rev.* **113**, 1046 (1959)
[4] M G Holland, *Phys. Rev.* **132**, 2461 (1963)
[5] M Asen-Palmer, K Bartkowski, E Gmelin, M Cardona, A P Zhernov, A V Inyushkin, A Taldenkov, V I Ozhogin, K M Itoh and E E Haller, *Phys. Rev.* **B56**, 9431 (1997)
[6] D T Morelli, J P Heremans and G A Slack, *Phys. Rev.* **B66**, 1953041 (2002)
[7] I G Kuleev and I I Kuleev, *JETP* **95(3)**, 480 (2002); **93(3)**, 649 (2002)
[8] S Simon, *Proc. R. Soc. (London)* **82**, 401 (1963)
[9] C Herring, *Phys. Rev.* **95**, 954 (1954)
[10] G A Slack and C Glassbrenner, *Phys. Rev.* **134**, A1058 (1964)
[11] T Ruf, R W Henn, M Asen-Palmer, E Gmelin, M Cardona, H J Pohl, G G Devyatych and P G Sennikov, *Solid State Commun.* **115**, 243 (2000)
[12] J R Olson, R O Pohl, J W Vandersande, A Zoltan, T R Anthony and W F Banholzer, *Phys. Rev.* **B47**, 14850 (1993)
[13] M D Tiwari and B K Agarwal, *Phys. Rev.* **B4(10)**, 3532 (1971)